PREPARATION AND CHARACTERIZATION OF THE SKUTTERUDITE-RELATED PHASE $Ru_{0.5}Pd_{0.5}Sb_3$

T. Caillat[a], J. Kulleck, A. Borshchevsky and J. -P. Fleurial

Jet Propulsion laboratory/California Institute of Technology
MS 277/207
4800 Oak Grove Drive
Pasadena, CA 91109
a) electronic mail: thierry.caillat@jpl.nasa.gov

Abstract

A new skutterudite phase $Ru_{0.5}Pd_{0.5}Sb_3$ was prepared. This new phase adds to a large number of already known materials with the skutterudite structure which have shown a good potential for thermoelectric applications. Single phase, polycrystalline samples were prepared and characterized by x-ray analysis, electron probe microanalysis, density, sound velocity, thermal expansion coefficient, and differential thermal analysis measurements. $Ru_{0.5}Pd_{0.5}Sb_3$ has a cubic lattice, space group $Im3(T_h^5)$, with a = 9.298 Å and decomposes at about 920 K. The Seebeck coefficient, the electrical resistivity, the Hall effect, and the thermal conductivity were measured on hot-pressed samples over a wide range of temperature. Preliminary results show that $Ru_{0.5}Pd_{0.5}Sb_3$ behaves as a heavily doped semiconductor with an estimated band gap of about 0,6 eV. The lattice thermal conductivity of $Ru_{0.5}Pd_{0.5}Sb_3$ is substantially lower than for the binary isostructural compounds $CoSb_3$ and $IrSb_3$. The potential of this material for thermoelectric applications is discussed.

1. INTRODUCTION

Skutterudite materials have generated a considerable interest as new thermoelectric materials over the past few years.[1,2] The value of a material for thermoelectric power generation or cooling applications is defined by the thermoelectric figure of merit Z which is a function of the Seebeck coefficient (α), electrical resistivity (p), and thermal conductivity (λ), and is defined as $Z = \alpha^2/\rho\lambda$. Skutterudite materials have interesting transport properties, in particular high hole mobilities.[3,4] The work on skutterudites initially started by the study of the properties of the binary compounds $IrSb_3$ and $CoSb_3$.[1-3] Although the binary compounds have good electrical properties, their

thermoelectric figure of merit is limited by their relatively high thermal conductivity (about 110 mW $cm^{-1}K^{-1}$ at room temperature for $IrSb_3$ and $CoSb_3$). If the lattice thermal conductivity of the binary compounds could be significantly reduced, high thermoelectric figure of merit values might be possible.[1]

Several approaches have already been considered to reduce the lattice thermal conductivity in this class of materials. The first approach, used for many state-of-the-art thermoelectric materials, is to form solid solutions between isostructural compounds and reduce the lattice thermal conductivity by increasing the point defect scattering. The preparation and characterization of p-type $Ir_xCo_{1-x}Sb_3$ solid solutions have been studied[5] and the results have shown that a reduction of about 70°/0 is achieved for a solid solution with about 12 mole% of $CoSb_3$. Another approach which has been considered to lower the lattice thermal conductivity of skutterudite materials is to study the so-called filled skutterudites. in these materials, a rare element R is inserted in the voids of the unfilled structure resulting in the formula RM_4B_{12} where M= Fe, Ru or 0s and B= P, As or Sb. This clement would substantially scatter the phonons, resulting in low thermal conductivity values. A recent study of the properties of the filled skutterudite $CeFe_4Sb_{12}$ showed that low lattice thermal conductivity values can be obtained for such materials.[6] 1 Iowever, more work is needed on these materials to improve their electrical properties and fully assess their potential for thermoelectric applications.

$CoAs_3$, which was first investigated by Oftedal,[7] is the prototype of the skutterudite structure. The skutterudite class of materials consists of compounds of the form AB_3 where A is Co, Rh, or lr, and B is P, As, or Sb. In addition to these binary compounds and filled skutterudites, several ternary skutterudite-related phases were reported in the literature and are listed in Table 1. These ternary skutterudite-related phases arc obtained by substitution of the transition-metal or pnicogen atom in a binary skutterudite by elements on the left and on the right of this atom similarly to diamond-like semiconductors.[8] The resulting phases are isoelectronic to the binary compounds. All the phases listed in Table 1 are derived from binary skutterudite compounds, the condition being that the valence-electron count remains constant. The substitution can occur on the anion site ($CoAs_3$ gives for example $CoGe_{1.5}Se_{1.5}$) or on the cation site ($CoSb_3$ gives for example $Fe_{0.5}Ni_{0.5}Sb_3$). Structurally related skutterudite phases can also be formed by partial substitution of the cation or the anion ($IrSb_3$ gives for example $PtSn_{1.2}Sb_{1.8}$). Almost no information is available in the literature about the transport properties of these ternary skutterudite phases. Because of the additional atomic disorder introduced, one can expect some reduction in the lattice thermal conductivity for these materials. Wc started to investigate the transport properties of these skutterudite materials to assess their potential for thermoelectric applications. A new ternary-related phase, $Ru_{0.5}Pd_{0.5}Sb_3$, obtained by substitution of Ru and Pd for Rh in the binary skutterudite compound $RhSb_3$ was prepared. We report here on the preparation and characterization of this new phase.

11. EXPERIMENTAL DETAILS

Single phase, polycrystalline samples of $Ru_{0.5}Pd_{0.5}Sb_3$ were prepared by direct synthesis of the elements. Ruthenium (99.9970/0), palladium (99.9°/0) and antimony (99.9999%) powders were mixed in stoichiometric ratio in a plastic vial before being loaded in a steel dic where they were compressed into dense cylindrical pellets. The pellets were scaled in a quartz ampoule under vacuum (10-5 Torr) which was heated for 8 days at about 870 K (lower than any of the melting point of the elements). The product was then removed from the ampoule, crushed, ground in an agate mortar and loaded again in a second quartz ampoule and heated for another 4 days at the same temperature.

Products of the annealings were removed from the ampoules and ground to a fine powder with an agate mortar and pestle. Silicon was added as an internal reference to compensate for variations in sample positioning and diffractometer calibration errors. X - ray diffraction analysis was accomplished using a Siemens D-500 diffractometer equipped with a Ni filter, Cu anode x-ray tube. The scattered x-rays were detected with a Kevex energy-dispersive spectrometer. The detector window was 380 eV and centered on Cu-K_α radiation. The dominant responses were used to characterize the 2Θ positions of the peaks observed in the detailed spectrum shown in Fig. 1. That pattern was taken with scan steps of **0.02** degrees 2Θ and integrated for 5 seconds pcr step. A computer program was used to provide a consistent least squares fit of the 31 peak data set to a face-centered cubic lattice structure. [14]

Several samples of $Ru_{0.5}Pd_{0.5}Sb_3$ were prepared by hot-pressing the prereacted powders in graphite dies. The hot-pressing was conducted at a pressure of about 20,000 psi and at a temperature of 770 K for about 4 hours. The density of the samples was measured by the immersion technique using toluene as liquid. The experimental density of the hot-pressed pellets was found to be about 96 % of the x-ray density value of 7.746 g cm^{-3}. The microstructure of the samples, polished by standard metallographic techniques, was investigated using an optical Nikon microscope under both ordinary and polarized light. The microprobe analysis of selected samples was performed on a JEOL JXA-733 superprobe. The examinations of polished hot-pressed pellets under a microscope showed that the samples were single phase. The microprobe analysis of the same samples also showed that the samples were single phase with a composition c1osc to $Ru_{0.5}Pd_{0.5}Sb_3$. Samples were also prepared for differential thermal analysis (DTA) measurements. A Du Pent 1600 DTA apparatus was used. The samples were sealed under 10-5 Torr vacuum in quartz capsules 5 mm in diameter and 15 mm long. The rounded bottom of the capsule was flattened and thinned by grinding and fire polishing to provide a better contact between the material and the thermocouple. Argon was used as the purge gas and heating rates of 2K $min.^{-1}$ were used. The temperatures recorded by DTA were determined with an accuracy of about ± 10 K. The shear and longitudinal sound velocity were measured at room temperature on samples about 8 mm long and using a frequency of 5 Mhz. The thermal expansion coefficient was measured on the same samples using a standard dilatometer apparatus.

Resistivity and 1 Iall effect measurements were conducted on selected samples between 80 and about 800 K. The high temperature resistivity (ρ) was measured using the van dcr Pauw technique with a current of 100 m A using a special high temperature apparatus.[15] The I Hall coefficient (R_H) was measured in the same apparatus with a constant magnetic field value of 8000 Gauss. The I Ian coefficient and resistivity were measured simultaneous] y between 80 and 350K using an automated low temperature I Hall effect apparatus equipped with a Joule-Thompson cooler. The carrier density was calculated from the 1 Iall coefficient, assuming a scattering factor of 1 in a single carrier scheme, by $p = 1/R_H c$ where p is the density of holes and e is the electron charge. The 1 Iall mobility (μ_H) was calculated from the I Ian coefficient and the resistivity values by $\mu_H = R_H/\rho$. The error was estimated at ± 0.5% and ± 2% for the resistivity and I Ian coefficient measurements, respectively. The Seebeck coefficient of the samples was measured on the same samples used for resistivity and 1 Iall coefficient measurements using a high temperature light pulse technique.[16] The error of measurements of the Seebeck coefficient was estimated to be less than ± 1%. The thermal conductivity of the samples was calculated from the experimental density, heat capacity and thermal diffusivity. The heat capacity and thermal diffusivity were measured using a flash diffusivity technique[17] and the overall error in the thermal conductivity measurement was about ± 10O/O.

111. RESULTS ANI) DISCUSSION

The x-ray analysis of the reacted powders showed that the samples were single phase. The experimental x-ray spectrum could be indexed on the basis of a cubic unit cell with the reflections corresponding to the skutterudite structure, space group $Im3 (T_h^5)$. The experimental x-ray pattern for sample 1RPS411P is shown in Figure 1 and the corresponding peak intensities and positions are tabulated in Table 11. The calculated room temperature lattice constant is a.== 9.298 ± 0.01 Å. This is slightly larger than for the binary compound $RhSb_3$ (a. = 9.2322 Å [9]) from which $Ru_{0.5}Pd_{0.5}Sb_3$ is derived. A similar finding was obtained for $Fe_{0.5}Ni_{0.5}Sb_3$ (a. = 9.0904 Å[10]), derived from the binary compound $CoSb_3$ (a. = 9.0345 ~Å).

The properties of $Ru_{0.5}Pd_{0.5}Sb_3$ are summarized in Table III and arc compared to the binary compounds $CoSb_3$ and $IrSb_3$. A temperature decomposition of 920 ± 10 K was found by DTA for $Ru_{0.5}Pd_{0.5}Sb_3$. Prolonged exposures of the samples at temperatures above 920 K resulted in substantial Sb losses. Microprobe analysis of samples heat-treated above the decomposition temperature showed that the composition of the resulting phase was close to $Ru_{0.5}Pd_{0.5}Sb_2$. We measured a thermal expansion coefficient of 9.09 x 10^{-6} K for $Ru_{0.5}Pd_{0.5}Sb_3$. This is to be compared to a value of 6.36 x 10^{-6} K for $CoSb_3$ and 6.6 x 10^{-6} K for $IrSb_3$ (see Table Ill).

The room temperature thermoelectric properties of $Ru_{0.5}Pd_{0.5}Sb_3$ (sample 1RPS4IIP) arc shown in Table III. Typical properties for the binary compound $CoSb_3$ and $IrSb_3$ arc also shown for comparison. Several samples were prepared but only slight differences in the properties were found. Hall coefficient measurements showed that all

hot-pressed samples had p-type conductivity at room temperature with a large hole density. The room temperature carrier density is 1.57 x 1020 cm^{-3} for sample 1RPS4HP. The electrical resistivity at room temperature is 0.476 x $10^{-3}\ \Omega$ cm and the Hall mobility 74 $cm^2\ V^{-1}s^{-1}$. As expected, the carrier mobility is significantly decreased in the ternary compound but is still reasonably large at this doping level. The Seebeck coefficient values arc relatively small with a room temperature value of 14 $\mu V\ K^{-1}$.

The electrical resistivity and Hall coefficient values are shown in Figures 2 and 3, respectively. The Hall coefficient values are positive and small. The Hall coefficient is practically temperature independent at low temperatures where extrinsic conduction occurs up to about 500K where the onset of intrinsic conduction is observed. With increasing temperature, the thermal excitation of electrons becomes larger and the Hall coefficient decreases. Above 500K, the Hall coefficient shows an energy activated behavior. A high temperature band gap of about 0.6 eV was estimated for $Ru_{0.5}Pd_{0.5}Sb_3$ from the slope of the quasi-linear variations of the 1 Iall coefficient in this temperature range. This is to bc compared with a high temperature band gap of about 0.8 eV for $RhSb_3$ and 0.55 CV for $CoSb_3$.[4] The electrical resistivit y increases with temperature over the entire temperature range of measurements. In Figure 4 we plot the Hall mobility as a function of the temperature. The data can be divided into two regions: (1) a gentle fall from 80 to about 400K and (2) a sharper fall from 400 to 800K. The mobility reasonably follows a $T^{-0.25}$ law below 400K and tends to follow a $T^{-3/2}$ above this temperature as shown in Figure 4. Therefore, it seems that the dominant scattering mechanism at high temperatures is acoustic phonons as indicated by the $T^{-3/2}$ law. In heavily doped semiconductors, the mobility is temperature independent for ionized impurity and neutral impurity scattering.[19] The variations of the Hall coefficient below 400K suggest that the samples arc strongly degenerated and that most of the impurities are ionized. The Hall mobility varies as $T^{-0.25}$ at low temperatures which indicates that a mixed carrier scattering mechanism operates. The small temperature dependence of the Hall mobility at low temperatures suggests that ionized impurity should be considered in this temperature range. We shall assume in the rest of the discussion that the scattering mechanism is dominated by a combination of acoustic phonons and ionized impurity below 400K and acoustic phonons above this temperature.

in Figure 5, the Seebeck coefficient values are plotted as a function of temperature. The Seebeck coefficient increases with increasing temperature up to about 700K and tends to flatten at higher temperatures. This is due to increasing thermally excited minority carriers which tend to decrease the magnitude of the Seebeck coefficient. In a single band model and considering a mixed scattering mechanism by acoustic phonon and ionized impurity, the Seebeck coefficient can be expressed as:

$$\alpha = + \frac{k}{c}\left\{\frac{\phi_4(\xi,b)}{\phi_3(\xi,b)} - \xi\right\} \qquad (1)$$

where *k is* the Boltzmann's constant, *e* is the electron charge, ξ is the reduced Fermi level, b is a measure of the relative strengths of ionized impurity and lattice scattering, and ϕ_x is a Fistul integral.") This formalism is particularly useful when mixed scattering mechanism occurs which is the case for $Ru_{0.5}Pd_{0.5}Sb_3$. Using the same formalism, the Hall coefficient (R_H) can be expressed as:

$$R_H = \frac{3h^3}{8\pi e(2m^*kT)^{3/2}} \frac{\phi_{9/2}(\xi,b)}{\phi_3(\xi,b)^2} \qquad (2)$$

where m* is the hole effective mass, *h is* the Planck's constant and T is the temperature in K. *b*=0 for acoustic phonon scattering and *b*= 10 for ionized impurity scattering. Based on the variations of the 1 Iall mobility below 400K, *b* will be taken equal to 8 in this temperature range. For temperatures above 400K, *b* will be taken equal to O. The reduced Fermi level can be calculated from the experimental Seebeck coefficient data using equation (1). The calculated reduced Fermi level values can then bc used in equation (2) to calculate the effective mass *m**. We calculated a room temperat ure effective mass of 0.28 m_0 for p-type $Ru_{0.5}Pd_{0.5}Sb_3$. This value is comparable to the values Of $0.17 m_0$ and 0.153 m. obtained for p-type $IrSb_3$ and $CoSb_3$, respectively (see 'l'able 11 l). The dashed line in Figure 4 represents the model calculation of the Seebeck coefficient using equation (1). The model describes reasonably well the experimental data.

The thermal conductivity data are shown in Figure 6 for several p-type $Ru_{0.5}Pd_{0.5}Sb_3$ samples and also for typical p-type $CoSb_3$. The data agree reasonably well for all the three $Ru_{0.5}Pd_{0.5}Sb_3$ samples measured but the slight differences observed are mainly due the differences in the sample density. The room temperature thermal conductivity is about 30 $mW\,cm^{-1}\,K^{-1}$, about three times lower than for p-type $CoSb_3$. In p-type $CoSb_3$, the predominant scattering mechanism above 10K is phonon-phonon umklapp.[3] For $Ru_{0.5}Pd_{0.5}Sb_3$, the thermal conductivity is almost temperature independent which indicates that, as expected, that additional scattering mechanisms occur. Because the samples are heavily doped, the electronic contribution (λ_e) to the total thermal conductivity (λ) becomes significant. This contribution can be calculated using the Wiedemann-Franz law:

$$\lambda_e = LT/\rho \qquad (3)$$

where *L* is the Lorenz number. Similarly to the Hall coefficient and Seebeck coefficient, the Lorenz number can be expressed as:

$$L = \frac{k^2}{e^2} \frac{\phi_3(\xi,b)\phi_5(\xi,b) - \phi_4(\xi,b)^2}{\phi_3(\xi,b)^2} \qquad (4)$$

The reduced Fermi level values, obtained from the experimental Seebeck coefficient values using equation (1), were used to calculate the Lorenz number. λ_e was then calculated as a function of temperature from the calculated Lorenz numbers and the experimental resistivity data. The result is shown in Figure 6 where the dashed line represents the lattice thermal conductivity of sample 1 RPS4H P. At room temperature, the electronic component accounts for about one third of the total thermal conductivity and the room temperature lattice thermal conductivity y is about 20 mW $cm^{-1}K^{-1}$, about five times lower than for p-type $CoSb_3$. The substitution of Ru and Pd to Rh in $RhSb_3$ is expected to create mass and volume disorder in the structure, resulting in lower thermal conductivity. Ru and Pd have only slightly different atomic masses and atomic radii. Therefore, the large decrease in lattice thermal conductivity is unlikely to be solely due to mass and volume fluctuations. The scattering of phonons by holes (or electrons) in heavily doped semiconductors can result in a substantial reduction of the lattice thermal conductivity. Our samples are heavily doped and phonon-hole scattering might also account for the low lattice thermal conductivity values.

The lattice thermal conductivity can be estimated using the formalism developed by Slack and Tsoukala.[2] The theoretical lattice thermal conductivity $\lambda'(\Theta)$ at the Debye temperature is given by:

$$\lambda'(\theta) = \frac{B\,\bar{M}\,\delta\,\theta^2}{n^{2/3}\,\gamma^2} \qquad (5)$$

where $\bar{M}$ is the average mass of an atom of the crystal, δ^3 is the average volume occupied by an atom, Θ is the Debye temperature, n is the number of atoms per unit cell, γ is the Grüneisen constant at $T=\Theta$, and $B = 3.04 \times 10^7\ S^{-3}K^{-3}$. For $Ru_{0.5}Pd_{0.5}Sb_3$, M = 117.2 g, and n = 32. The Debye temperature can be calculated from the mean sound velocity which can be estimated from the experimental longitudinal (v_l) and shear (v_s) sound velocity listed in Table III.[20] The mean sound velocity v_m is given by:

$$v_m = \left(\frac{1}{3}\left[\frac{2}{v_s^3} + \frac{1}{v_l^3}\right]\right)^{-1/3} \qquad (6)$$

We calculated a mean sound velocity of 2.652×10^5 cm s^{-1}. The Debye temperature is related to the mean sound velocity by the equation:

$$\Theta = \frac{h}{k}\left[\frac{3n}{4\pi}\frac{Nd}{M}\right]^{1/3} v_m \qquad (7)$$

where h and k are the Planck's and Botlzmann's constants, respectively, N is the Avogadro's number, d is the density, and M' is the molecular weight of the solid. We calculated a Debye temperature of 269K for $Ru_{0.5}Pd_{0.5}Sb_3$. The Deb yc temperature is 308 and 307K for $IrSb_3$ and $CoSb_3$, respectively (see Table 111). Finally, a Grüneisen constant

of 1.21 was calculated for $Ru_{0.5}Pd_{0.5}Sb_3$ using the formalism developed by Slack and Tsoukala.[2] The Grüneisen constant for $IrSb_3$ and $CoSb_3$ is 1.42 and 0.95, respectively.[2,18]

The theoretical lattice thermal conductivity obtained for $Ru_{0.5}Pd_{0.5}Sb_3$ from equation (5) is 55 $mW\,cm^{-1}\,K^{-1}$ at room temperature. Using the same formalism we estimated a theoretical lattice thermal conductivity value of about 101 $mW\,cm^{-1}K^{-1}$ for p-type $CoSb_3$[18] and Slack and Tsoukala estimated a value of 94 $mW\,cm^{-1}K^{-1}$ for p-type $IrSb_3$.[2] Although the experimental and calculated theoretical values for the lattice thermal conductivity do not agree quantitatively, the results show that there is a significant decrease for $Ru_{0.5}Pd_{0.5}Sb_3$ compared to the binary compounds $IrSb_3$ and $CoSb_3$.

The calculated ZT values are low ($ZT_{max} \approx 0.02$ at 800K) mainly because of the high doping levels of the samples, resulting in low Seebeck coefficient values. Larger Seebeck coefficient values would likely be obtained for samples with smaller doping levels. The values of the effective mass for p-type $Ru_{0.5}Pd_{0.5}Sb_3$ are slightly larger than for p-type $CoSb_3$ and $IrSb_3$, suggesting that Seebeck coefficient values at least as large as for p-type $CoSb_3$ and $IrSb_3$ can be obtained for p-type $Ru_{0.5}Pd_{0.5}Sb_3$. The optimization of the doping level might be achieved by doping, for example. The lattice thermal conductivity is small and ZT values comparable to state-of-the-art thermoelectric materials might be possible with optimization of the doping levels.

IV. CONCLUSION

We studied for the first time the thermoelectric properties of a new ternary skutterudite material: $Ru_{0.5}Pd_{0.5}Sb_3$. The results showed that this compound behaves as a heavily doped semiconductor. The thermal conductivity in this compound is substantially reduced compared to binary compounds such as $CoSb_3$ or $IrSb_3$. The results suggest that, by optimizing the doping level, ZT values comparable to state-of-the-art thermoelectric materials might be possible. Further studies should aim to investigate the effect of various impurities in this compound in order to optimize the doping level and fully assess its potential for thermoelectric applications. Other ternary compounds will be investigated as well to further study the good potential of these materials for thermoelectric applications.

ACKNOWLEDGEMENTS

The work described in this paper was carried out at the Jet Propulsion Laboratory/California Institute of Technology, under contract with the National Aeronautics and Space Administration. We thank Dr. G. A. Slack for useful discussions on thermal condcutivity. The authors would like to thank Danny Zoltan and Andy Zoltan for thermoelectric properties measurements, Paul Carpenter for microprobe analyses, Phil Stevens for DTA experiments, and Yoseph Bar-Cohen for sumd velocity measurements.

TABLE CAPTIONS

Table 1. Ternary skutterudite materials reported in the literature

Table 11. Experimental X-ray data for $Ru_{0.5}Pd_{0.5}Sb_3$

Table 111. Some properties at room temperature for p-type $IrSb_3$[2], p-type $CoSb_3$[18], and p-type $Ru_{0.5}Pd_{0.5}Sb_3$ (this study).

FIGURES CAPTIONS

Figure 1. Experimental x-ray spectra of $Ru_{0.5}Pd_{0.5}Sb_3$. The numbers correspond to the peak numbers listed in Table II.

Figure 2. Electrical resistivity versus inverse temperature for two hot-pressed $Ru_{0.5}Pd_{0.5}Sb_3$ samples.

Figure 3. 1 Hall coefficient versus inverse temperature for two hot-pressed $Ru_{0.5}Pd_{0.5}Sb_3$ samples.

Figure 4. I Hall mobility versus temperature for two hot-pressed $Ru_{0.5}Pd_{0.5}Sb_3$ samples.

Figure 5. Seebeck coefficient versus temperature for two hot-pressed $Ru_{0.5}Pd_{0.5}Sb_3$ samples. The dashed line represents a model calculation assuming a single valence band with both acoustic and ionized impurity carrier scattering between 300 and 400K, and only acoustic phonon scattering above this temperature.

Figure 6. Thermal conductivity versus temperature for several hot-pressed $Ru_{0.5}Pd_{0.5}Sb_3$ samples. The solid line corresponds to the typical thermal conductivity values for p-type $CoSb_3$[3] and the dashed line is the calculated lattice thermal conductivity for sample 1 RPS4HP.

REFERENCES

1. T. Caillat, A. Borshchevsky, and J. -P. Fleurial, in Proceedings of the X1th international Conference on Thermoelectric, University of Texas at Arlington, 1992, edited by K. R. Rao (University of Texas at Arlington Press, Arlington), 98 (1993).
2. G. Slack and V. G. Tsoukala, J. Appl. Phys. 76, 1665 (1 994).
3. D. T. MorelIi, T. Caillat, J. -P. Fleurial, A. Borshchevsky, J. Vandersande, B. Chen, and C. Uher, Phys. Rev. B 51, 9622(1 995).
4. T. Caillat, J. -P. Fleurial , and A. Borshchevsky, J. Cryst. Growth accepted for publication (1995).
5. A. Borshchevsky, J. -P. Fleurial, E. Allevato., and T. Caillat, in Proceedings of the XIIIth International Conference on Thermoelectrics, Kansas City, MO, USA, edited by B. Mathiprakasam and P. Heenan (AIP Conference 316, New York), 31 (1995).
6. D. T. Morelli and G. P. Meisner, J. Appl. Phys. 77, 3777 (1 995).
7. 1. Oftedal, Z. Kristallogr. 6,517 (1928).
8. N. A. Goryunova, *Chemistry of Diamond-Like Semiconductors*, MIT Press (1965).
9. R. Korenstein, S. Soled, A. Weld, and G. Collin, Inorg. Chem. 16, 2344(1977).
10. A. Kjekshus and T. Rakke, Acts Chem. Stand. A28,99(1974).
11. A. Lyons, R. P. Gruska, C. Case, S. N. Subbarao, and A. Weld, Mat. Res. Bul. **13**, 125 (1978).
12. C. M. Pleass and R. D. Heyding, Canadian Journal of Chemistry 40, 590(1962).
13. S. Bahn, T. Gödecke, and K. Schubert, J. of Less-Common Met. 19, 121 (1 969).
14. J 1. T. Evans Jr., D.E. Appleman, and D.S. Handwerker, Report#PB216 188, U.S. Dept. of Commerce, National Technical information Center, 5285 Port royal Road, Springfield, VA 22151 (1973).
15. J. A. McCormack and J. -P. Fleurial, in *Modern Perspectives on Thermoelectric and Related Materials,* edited by D. D. Aired, C. B. Vining and G. A. Slack, Materials Research Society, Pittsburgh, p. 135 (1991).
16. C. Wood, D. Zoltan and G. Stapfer, Rev. Sci. Instrum. S6, 179 (1 985).
17. J.W. Vandersande, C. Wood, A. Zoltan, and D. Whittenberger , *Thermal Conductivity,* Plenum Press, New York, 445 (1 988).
18. T. Caillat, J. -P. Fleurial , and A. Borshchevsky (unpublished).
19. V. 1. Fistul, *Heavily Doped Semiconductors* (Plenum Press, New York, 1969).
20. O. L. Anderson, J. Phys. Chem. Solids 24, 909(1 963).

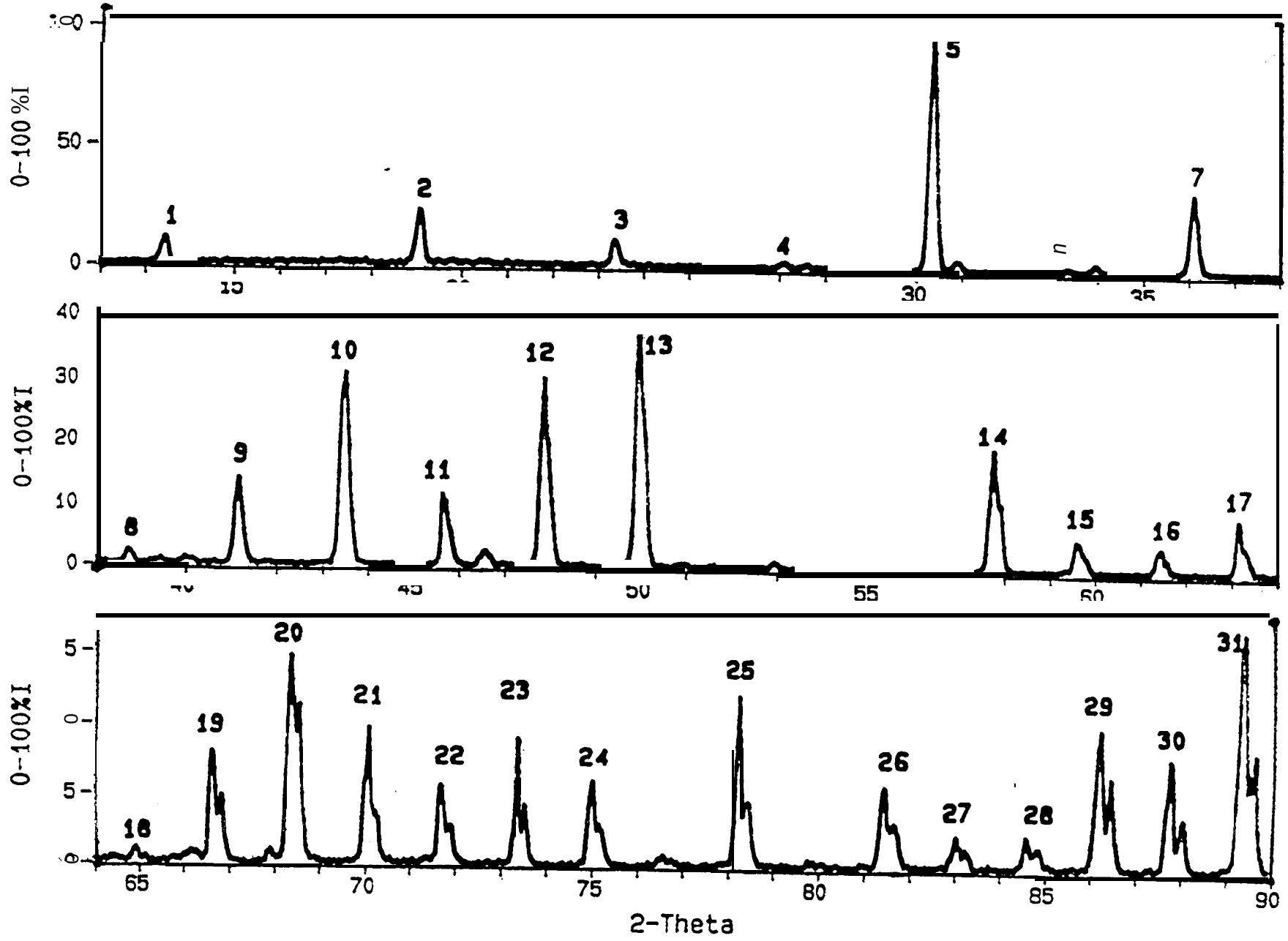
0-100 %I
0-100%I
0-100%I
1
2
3
4
5
7
8
9
10
11
12
13
14
15
16
17
18
19
20
21
22
23
24
25
26
27
28
29
30
31
2-Theta

Figure (1)

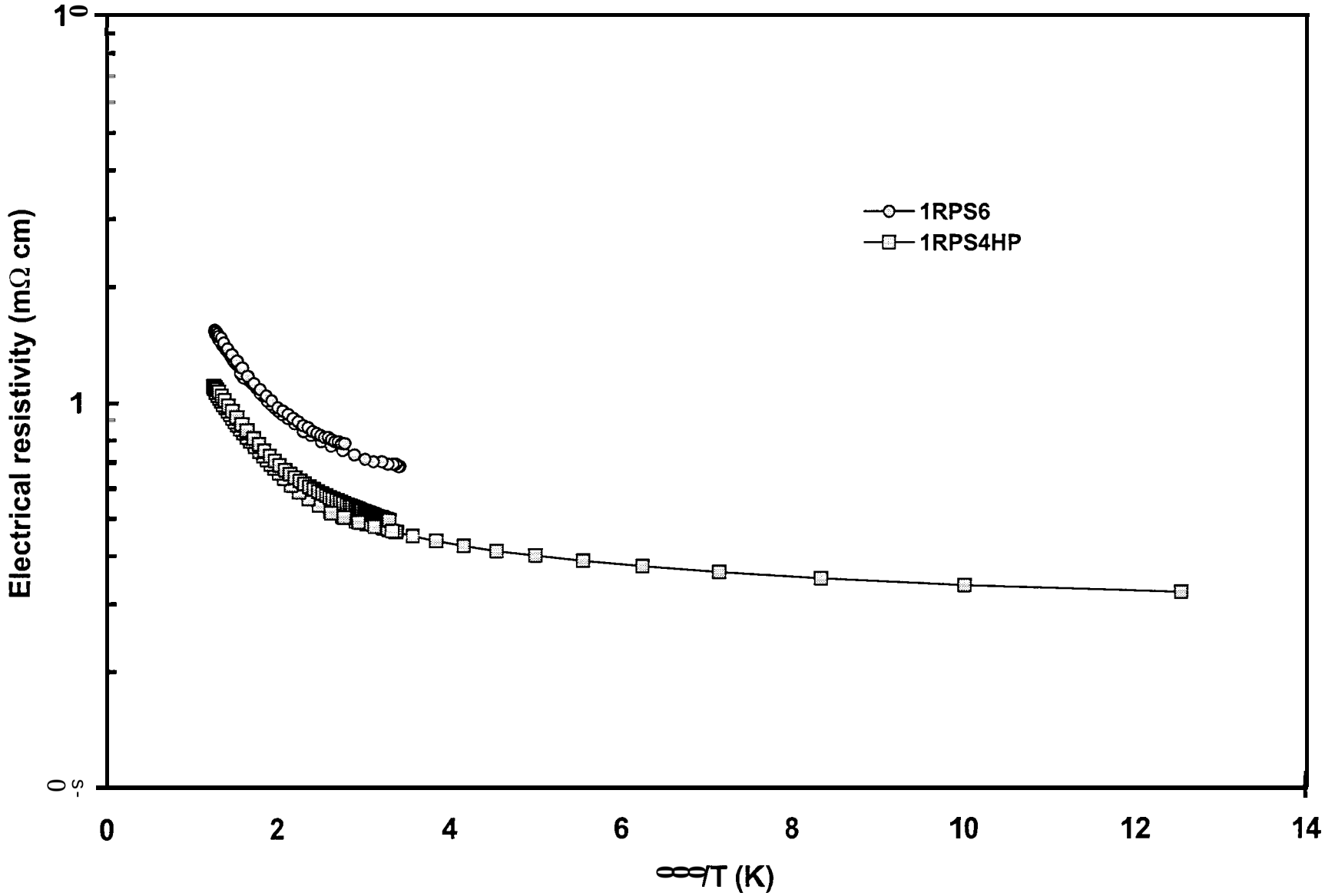
Electrical resistivity (mΩ cm)
1
0
0
2
4
6
8
10
12
14
T (K)
1RPS6
1RPS4HP

Figure 2

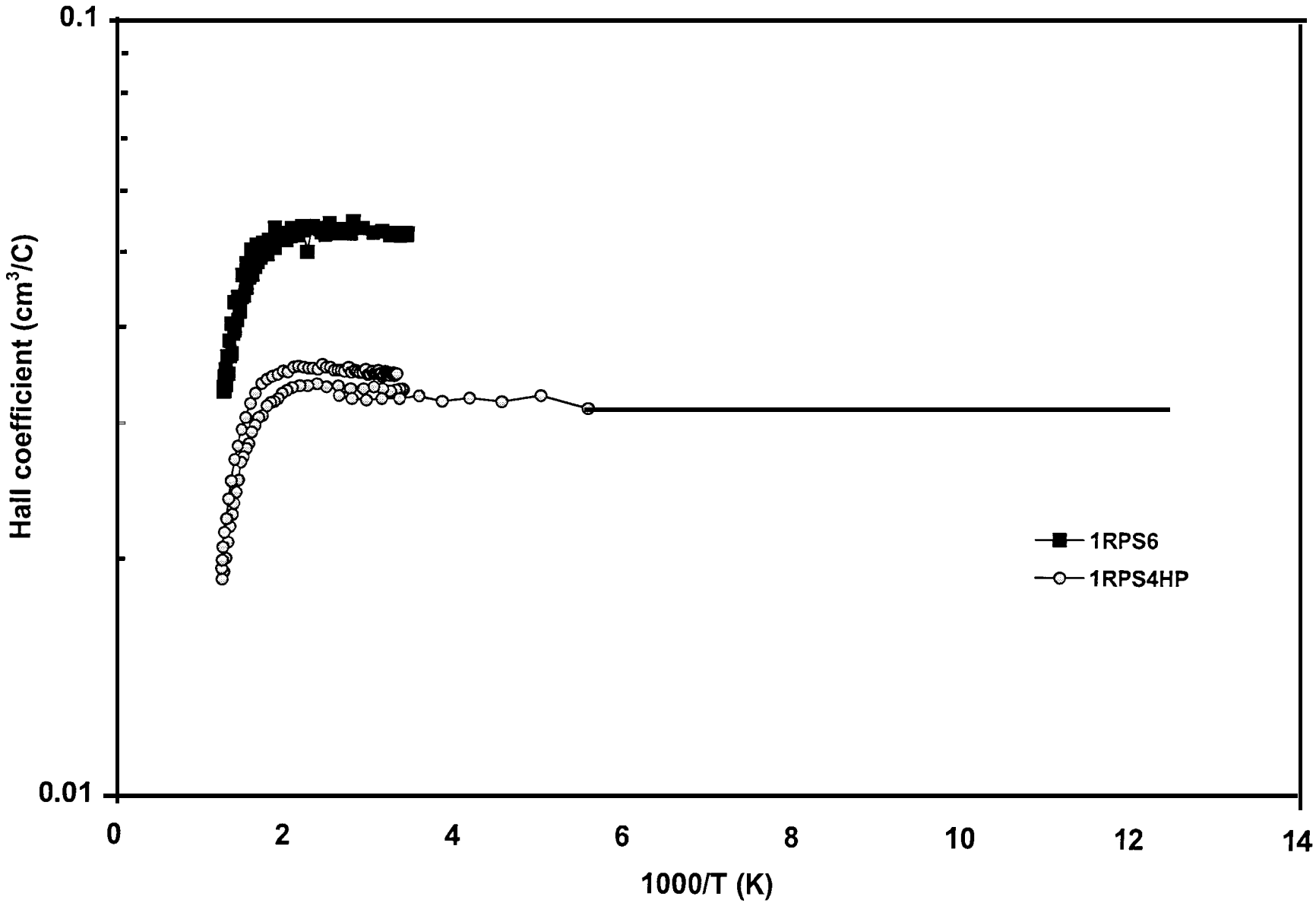
0.1
0.01
Hall coefficient (cm3/C)
0
2
4
6
8
10
12
14
1000/T (K)
1RPS6
1RPS4HP

Figure 3

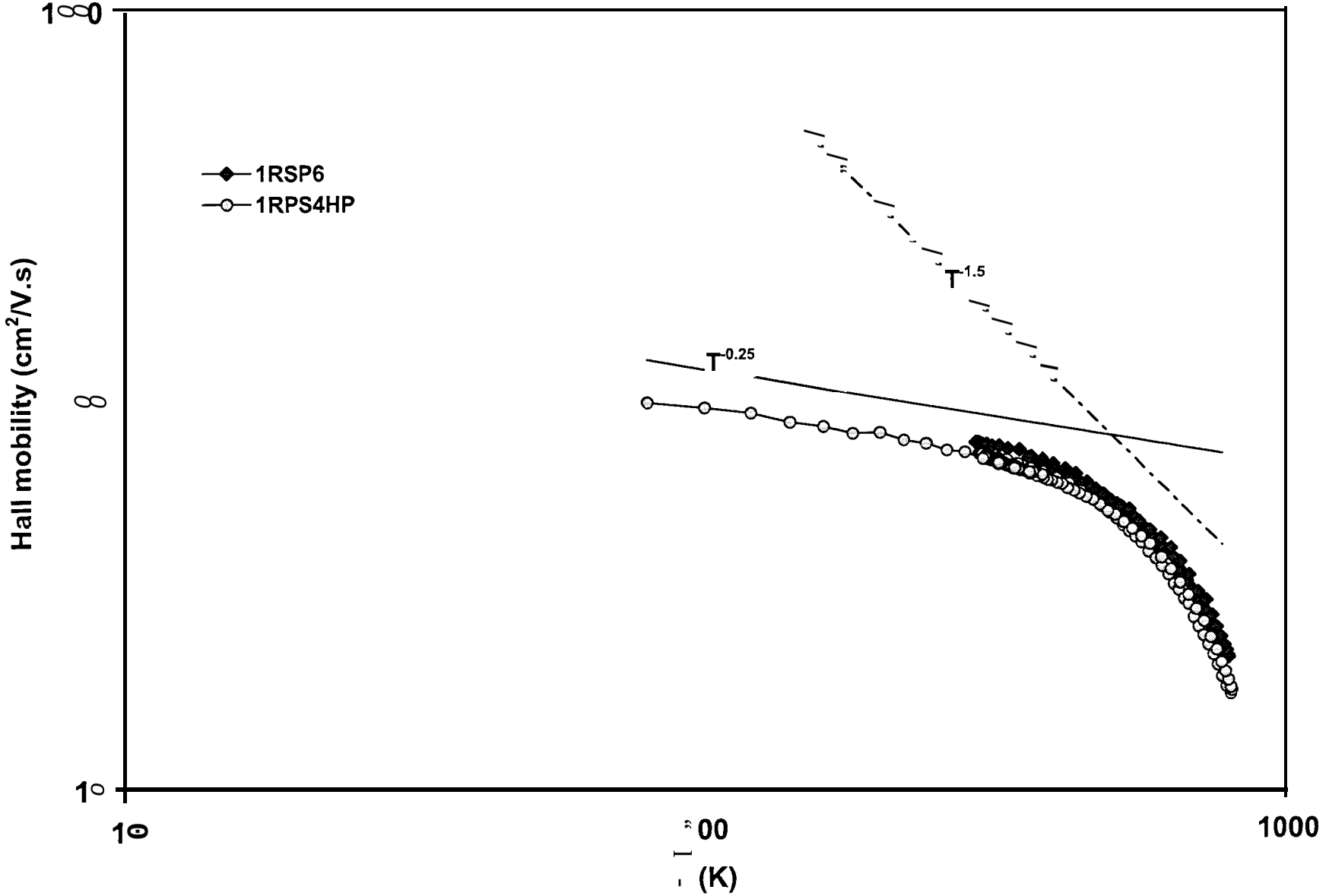

Figure 4

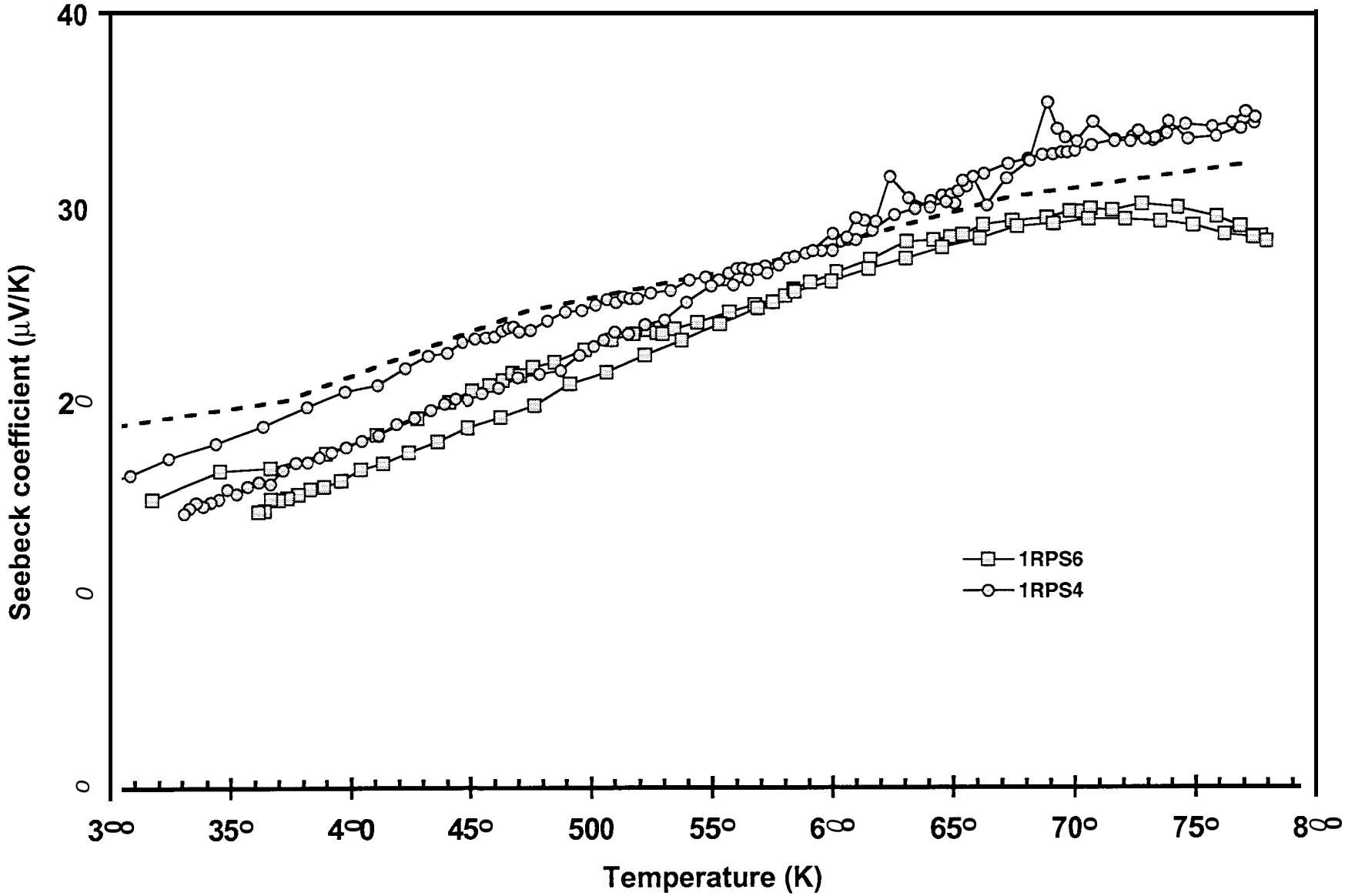
40
30
20
0
0
Seebeck coefficient (μV/K)
1RPS6
1RPS4
Temperature (K)

Figure 5

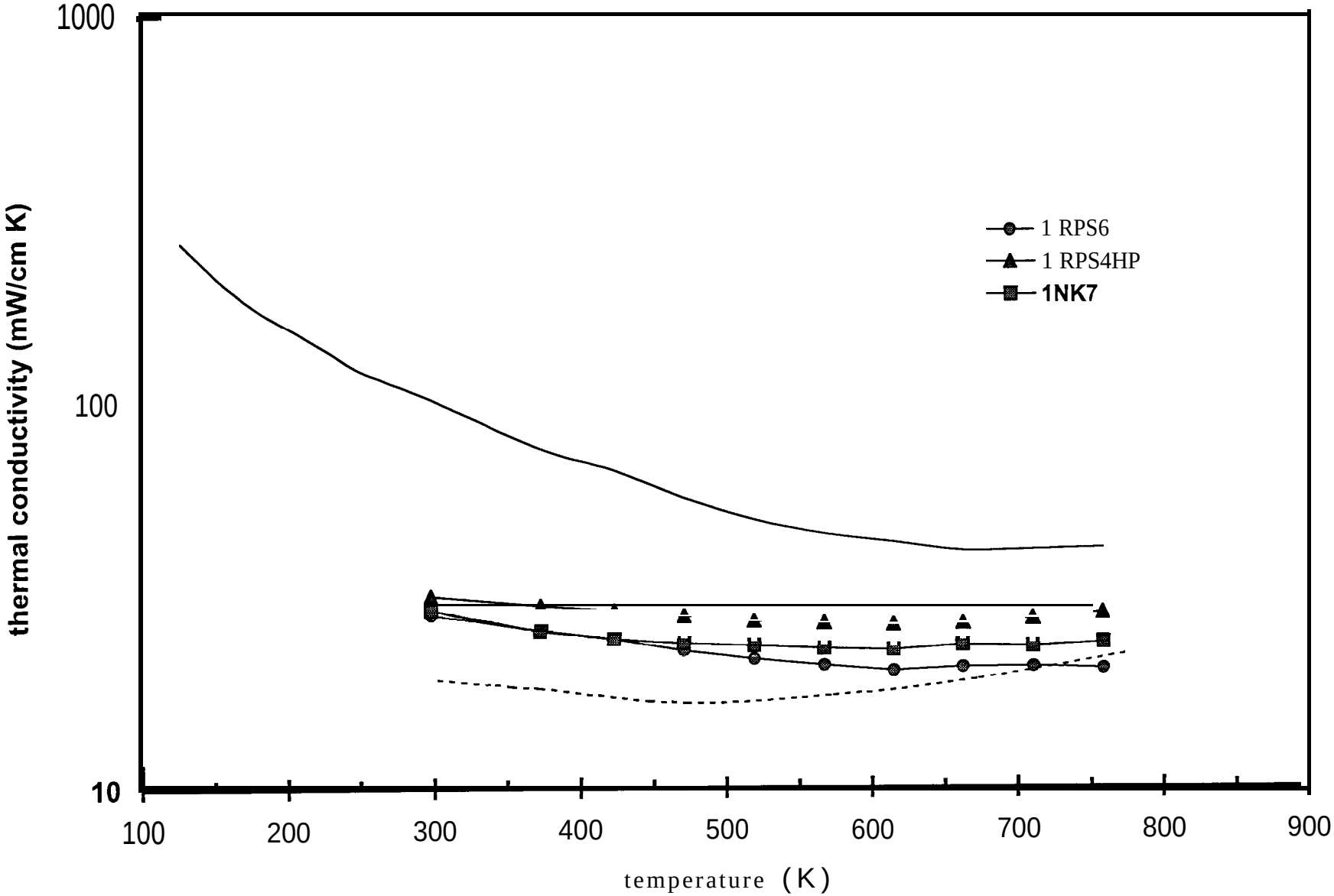
1000
100
10
thermal conductivity (mW/cm K)
1 RPS6
1 RPS4HP
1NK7
100
200
300
400
500
600
700
800
900
temperature (K)

Figure 6